Study on the dissipation mechanism of shock and vibration energy in a stress release area of deep roadway

Jianguo Ning, Jun Wang, Xuesheng Liu, Yunliang Tan

State Key Laboratory Breeding Base for Mining Disaster Prevention and Control, Shandong University of Science and Technology, Qingdao, China

Abstract

Stress release through artificial blasting is often used in deep roadways to prevent rock-burst, but the results in many coal mines are unsatisfactory since the dissipation mechanism of shock and vibration energy influenced by the rupture structure of the coal and rock mass in the stress release area is unclear. In this paper, the surrounding deep roadway rock is divided into three parts, which are the stress concentration area, the stress release area and the anchor area. The stress release area produced by artificial blasting consists of spherical rupture units, and these units can be divided into the crush zone, rupture zone and fracture zone from inside to outside. The attenuation coefficient of the high energy stress wave that propagates from the intact area and stress release area to the anchor area is obtained based on the simplified model of normal incidence impact energy. The numerical simulation method is used to research the dynamic variation of vertical stress, elastic strain energy and the plastic zone of the surrounding rock under the action of shock and vibration energy, and the dissipation law of shock and vibration energy in the stress release area is revealed. Field application shows that setting the stress release area artificially can reduce the impact of shock and vibration energy on the anchor supporting system and improve the rock-burst prevention capability of the anchor supporting system.

Keywords: deep roadway, rock-burst prevention, stress release area, shock and vibration energy, dissipation

1. Introduction

Mining depths are increasing along with the exploitation of coal resources in many counties, such as South Africa, Poland, Russia, Canada and Australia. The frequency and intensity of roadway rock-bursts increase significantly during the exploitation of deep resources, and statistics indicate that 85% of all rock-burst accidents occur in deep roadways [1]. Deep roadway rockbursts usually release energy in a sudden, sharp and violent form, destroys coal and rock mass and blocks the roadway, resulting in dumping and damage of supporting equipment and other equipment as well as heavy casualties. For a long time, the prevention of rock-bursts in deep roadways has been one of the major challenges in mining rock mechanics and has always been an important research topic in academic and engineering circles both at home and abroad [2-3].

Stress release by artificial blasting is a method often used to prevent rock-bursts in deep roadways [4-6]. It can destroy rocks and set a stress release area in the surrounding rock. The crushed coal and rock mass in the stress release area can release and dissipate shock and vibration energy, but the effect of the rupture structure of the coal and rock mass in the stress release area on the release and dissipation of shock and vibration energy is still unclear at this time, resulting in unsatisfactory outcomes in many coal mines.

2. The simplified model of normal incidence impact energy

After the excavation of a deep roadway, the stress state of the surrounding rock changes and a stress concentration area forms. When the anchor supporting system cannot resist the impact of high energy in the stress concentration area, this high energy may be released in a sudden, sharp and violent form, which will initiate a rock-burst. Commonly, a drilling rig is used to drill holes in the surrounding rock of the deep roadway, explosives are placed at the junction of the elastic zone and the plastic zone of these holes before sealing, and a stress release area is formed in the surrounding rock by artificial blasting. In order to prevent rock-burst, flexible energy absorbing devices, such as bolts and cables, are used outside the stress release area to form a supporting system, as shown in Fig. 1.

In the stress release area, the explosion of spherical charges causes disturbances to the surrounding rock and spreads outward in the form of a stress wave, which results in varying degrees of damage to the rock mass. The closer to the charges, the more serious the rock ruptures. The relevant literature shows that the rock mass around the charges can be divided into the crush zone, rupture zone and fracture zone from inside to outside [7]. The partition structure produced by the explosion of one single charge can be called a spherical rupture unit, as shown in Fig. 2. When many spherical charges are arranged in a certain order, these spherical rupture units will form a stress release area in the deep roadway, as shown in Fig. 3.

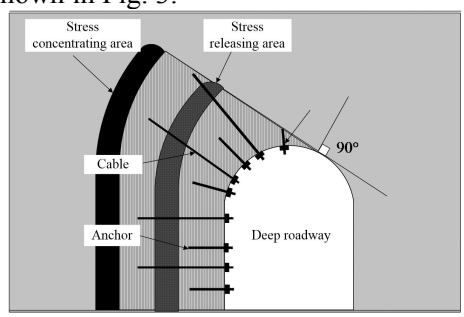

Fig. 1: 'Defense belt' model of rock-burst in deep roadway.

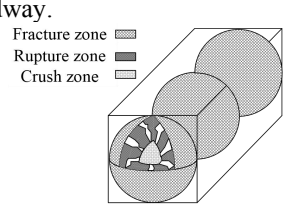

Fig. 2: Structure of spherical rupture unit and stress release area.

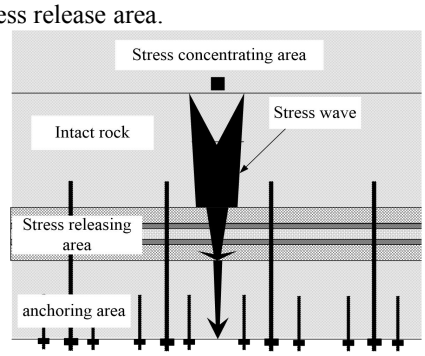

Fig. 3: Simplified attenuation model of stress wave energy in ideal rock.

For a single spherical rupture unit, shock and vibration energy in the deep roadway pass through the fracture zone, rupture zone and crush zone, and then back through the rupture zone and fracture zone and on to the supporting system. In order to facilitate analysis, we assume normal stress wave incidence at each

partition and eventual action on the supporting system, and we assume that the joint surfaces are smooth and perpendicular to the direction of the stress wave, as shown in Fig. 3.

3. Stress wave attenuation law in the intact area and the stress release area

3.1 Stress wave propagation and attenuation laws in the intact area

When the shock and vibration energy is disturbed, it will propagate in the form of a stress wave whose amplitude attenuates with the increase of propagation distance and time, which can be called space attenuation and time attenuation [8]. The governing equation of a longitudinal wave in a Kelvin viscoelastic body is

$$\rho_0 \frac{\partial^2 d}{\partial t^2} = E_V \frac{\partial^2 d}{\partial x^2} + \eta_V \frac{\partial^3 d}{\partial x^2 \partial t} \tag{1}$$

where E_V is the elastic modulus, η_V is the viscosity coefficient, σ is stress, ε is strain, t is time, d is displacement in the direction of x, and ρ_0 is the density of intact rock.

If the distance between a hypocenter and particle is x, based on harmonic equations, the attenuation of amplitude can be expressed as

$$d(x,t) = Ae^{i\left(\omega_q t - kx\right)} \tag{2}$$

where A is the amplitude, ω_q is the vibration frequency, k is the number of wave responses in the rock, and i is the imaginary unit.

On the basis of formula (1) and (2), the attenuation coefficients of amplitude with time and space in a Kelvin viscoelastic body are

$$\alpha_t = \frac{\eta_V E_V \omega_q^2}{4\left(E_V^2 + \eta_V^2 \omega_q^2\right)} \left(\sqrt{1 + \frac{\eta_V^2 \omega_q^2}{E_V^2}} + 1 \right) \tag{3}$$

$$\alpha_s^2 = \frac{\rho_0 E_V \omega_q^2}{2\left(E_V^2 + \eta_V^2 \omega_q^2\right)} \left(\sqrt{1 + \frac{\eta_V^2 \omega_q^2}{E_V^2}} - 1 \right) \tag{4}$$

Therefore, when the propagation distance and time in intact rock are L_1 and T respectively, the amplitude A_1 of the stress wave is

$$A_1 = A_0 \cdot e^{-\alpha_s L_1} \cdot e^{-\alpha_t T} \tag{5}$$

3.2 Stress wave transmission, reflection and attenuation law in the stress release area

When shock and vibration energy propagates to the stress release area, the stress wave exhibits complex phenomena of transmission and reflection among partitions which have a great effect on the propagation and attenuation of the stress wave in the rock mass [9]. As shown in Fig. 4, at the time of normal stress wave incidence at surface F_1 normally, the transmitted wave passes through the surface and refracts and reflects at surface F_2. The reflected wave then propagates back to surface F_1 and reflects again; this process will repeat.

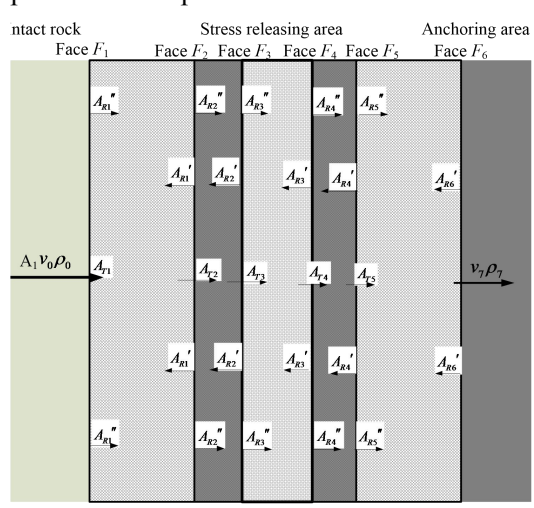

Fig. 4: Incidence and reflection of stress wave in stress release area.

If the wave velocity in the intact rock is v_0, the wave velocity in the fracture zone is v_1, the reflection coefficient of surface

F_1 when the stress wave propagates from the intact rock to the fracture zone is T_1; the reflection coefficient of surface F_1 when the stress wave propagates from the fracture zone to the intact rock is f_2; the reflection coefficient of surface F_2 when the stress wave propagates from the fracture zone to the rupture zone is f_1; the width of joint layer is Δr; and the wavelength is λ.

From reference [10], the number of stress wave reflections in the fracture zone depends on the ratio of the wavelength and the width of the joint layer.

$$n = \frac{v_1 \lambda}{v_0 \Delta r} \tag{6}$$

If the attenuation of the refracted wave that first passes through the joint layer is $(\Delta A_T)_1$, the stress wave that reflects n times at surfaces F_1 and F_2 (n is an even number) can be expressed as

$$A_R^{(n)} = f_1^{\frac{n}{2}} f_2^{\frac{n}{2}} [A_T + \sum_{i=1}^{n} (\Delta A_T)_1] \tag{7}$$

For a common rock mass, the stress wave can be expressed as

$$A_T = \frac{C}{r^{\alpha_s}} \tag{8}$$

where α_s is the space attenuation coefficient, r is the distance between stress wave A_T and the hypocenter, and C is a constant.

From formula (8), we obtain

$$(\Delta A_T)_n = C \cdot [\frac{1}{(r + n\Delta r)^{\alpha_s}} - \frac{1}{(r + (n-1)\Delta r)^{\alpha_s}}] \tag{9}$$

Then

$$\sum_{i=1}^{n} (\Delta A_T)_i = C \cdot [\frac{1}{(r + n\Delta r)^{\alpha_s}} - \frac{1}{r^{\alpha_s}}] \tag{10}$$

The wave superposed by n+1 stress wave forms in the stress release area after n (even) times' reflections. If $(\Delta A_T)_0 = 0$, from formula (6), we obtain $k\Delta r \le n\Delta r \le (v_q / v_p)\lambda$. For joints which are far from source, we have $r >> k\Delta r$, so $(r + k\Delta r) \approx r$. Therefore, the amplitude of the stress wave attenuated by the fracture zone is

$$A_2 = T_1 A_1 \sum_{k=0}^{\frac{n}{2}} f_1^k f_2^k \tag{11}$$

In the same way, the amplitude of the stress wave propagating into the anchor area through the fracture zone, rupture zone and crush zone is

$$A_3 = A_1 \frac{2^6}{\prod_{i=0}^{6} \left(1 + v_i \rho_i / v_{i+1} \rho_{i+1}\right)} \sum_{k=0}^{\frac{n}{2}} f_1^k f_2^k \sum_{k=0}^{\frac{n}{2}} f_3^k f_4^k \sum_{k=0}^{\frac{n}{2}} f_5^k f_6^k \sum_{k=0}^{\frac{n}{2}} f_7^k f_8^k \sum_{k=0}^{\frac{n}{2}} f_9^k f_{10}^k \tag{12}$$

where f_3, f_4, f_5, f_6, f_7, f_8, f_{10} are reflection coefficients of the stress wave propagating from the rupture zone to the crush zone at surface F_3, from the rupture zone to the fracture zone at surface F_2, from the crush zone to the rupture zone at surface F_4, from the crush zone to the rupture zone at surface F_3, from the rupture zone to the fracture zone at surface F_5, from the rupture zone to the crush zone at surface F_4 and from the fracture zone to the rupture zone at surface F_4 respectively, and f_9 is the refraction coefficient of the stress wave propagating from the fracture zone to the anchor area at surface F_6.

So, the attenuation coefficient of a stress wave with high energy propagating through intact rock and the stress release area to the anchor area is

$$A = A_0 \frac{2^6 e^{-\alpha_s L_1} \cdot e^{-\alpha_t T}}{\prod_{i=0}^{6} \left(1 + v_i \rho_i / v_{i+1} \rho_{i+1}\right)} \sum_{k=0}^{\frac{n}{2}} f_1^k f_2^k \sum_{k=0}^{\frac{n}{2}} f_3^k f_4^k \sum_{k=0}^{\frac{n}{2}} f_5^k f_6^k \sum_{k=0}^{\frac{n}{2}} f_7^k f_8^k \sum_{k=0}^{\frac{n}{2}} f_9^k f_{10}^k \quad (13)$$

4. Numerical simulation

4.1 Modeling and simulation scheme

The transformation process of energy in the surrounding rock under impact loading was studied with the background of the geological and mining conditions of No. 2304 air return roadway in the Tangkou coal mine. The depth of the roadway is 1000m, and the width and height are 4m and 3m respectively. Bolts, anchors and nets are used to support the roadway. The diameter and length of the roof bolts are 20mm and 2400mm respectively, and both row and line spaces are 800mm. The diameter and length of the roof cables are 17.8mm and 6000mm respectively, and the row and line spaces are 1200 mm and 2400mm respectively. The lithological and mechanical parameters of the roof and floor are shown in Table 1.

Table 1: Lithological and mechanical parameters of roof and floor.

Lithology	Thick-ness/m	Density /kN/m^3	Shear modulus /GPa	Bulk modulus /GPa	Cohesion /MPa	Tensile strength /MPa	Friction angle/°
Fine-grained sandstone	19.0	27.4	9.43	13.64	4	6	36
Gritstone	5.0	25.2	5.41	6.65	3.33	5.4	38
Coal	3.0	13. 4	1.52	4.22	2.4	1.0	18
Mudstone	1.0	2.0	25.8	11.43	13.4	5	7
Fine-grained sandstone	6.0	27.4	9.43	13.64	4	6	36

FLAC3D was used to build a computing model, the length, width and height of which were 52m, 10m and 34m respectively, and the width and height of the roadway were 4m and 3m respectively. On the top of the model, a load of 25MPa was exerted in the vertical direction and 32.25MPa was exerted in the horizontal direction. On the sides of the model, the displacement in both the x and y directions was fixed. On the bottom of model, the displacement in all directions was fixed. The impact load was exerted when stress reached a balance after the excavation of the roadway. Based on the research in reference [11], the impact hypocenter was simplified as a harmonic stress wave. The peak intensity of the stress was 40MPa, the frequency was 40Hz, the action time was 0.1 second, and the boundary was set as static. In order to obtain a contrast, two simulation schemes were designed.

Scheme one: the impact hypocenter was exerted on the roof about 27m above the top of the roadway after static force reached balance, and then dynamic calculation was performed.

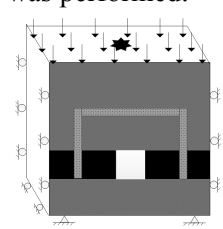

Fig. 5: Schematic diagram of stress release area.

Scheme two: the impact hypocenter was exerted on the roof about 24m above the top of the roadway and the stress release

area was set in the surrounding rock 12m~14m from the surface of the roadway after static force reached balance, as shown in Fig. 5, and then dynamic calculation was performed. Vertical stress, elastic strain energy and the plastic zone of the surrounding rock were monitored in the numerical calculations to analyze the effect of impact energy dissipation in the stress release area and reveal the impact energy dissipation law.

4.2 Impact energy dissipation law in the stress release area

The dynamic responses of vertical stress, elastic strain energy and the plastic zone of surrounding rock are shown in Fig. 6 ~ Fig. 10.

(1) Variation of vertical stress under impact energy.

The dynamic response of vertical stress under the action of impact energy is shown in Fig. 6~ Fig. 7. Under the action of impact energy (with impact time of 0~0.1 seconds), the vertical stress on the surrounding rock without a stress release area (Scheme one) is high and reaches 70MPa (0.06 seconds) in the roof 24m above the roadway, with a stress concentration factor of 2.8, while the stress is 40MPa (0.06 seconds) on the side about 20m from the roadway. In contrast, the vertical stress on the surrounding rock with a stress release area (Scheme one) is low and achieves its maximum (0.06 seconds) in the roof 24m above the roadway, about 65MPa with a 7% decrease. Additionally, the vertical stress on the surrounding rock between the stress release area and the surface of the roadway has the greatest decline, about 25%, and the highest vertical stress is about 30MPa (0.06 seconds).

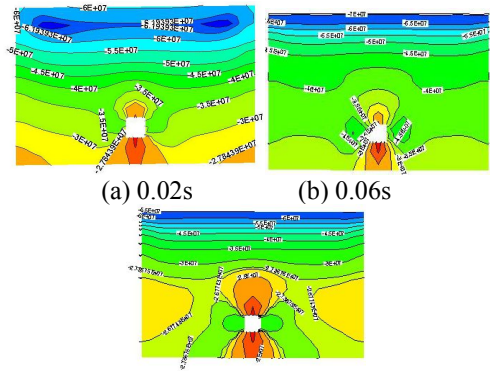

(a) 0.02s (b) 0.06s

(c) 0.1s

Fig. 6: Variation of vertical stress in Scheme one.

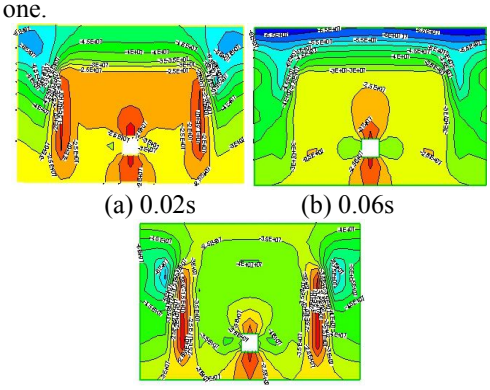

(a) 0.02s (b) 0.06s

(c) 0.1s

Fig. 7: Variation of vertical stress in Scheme two.

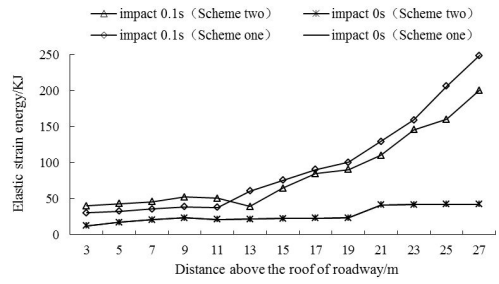

Fig. 8: Variation of elastic strain energy in the roof.

(2) Variation of elastic strain energy under impact energy.

The dynamic response of elastic strain energy under the action of impact energy is shown in Fig. 8. The elastic strain energy on the roadway roof without a stress release area (Scheme one) is higher, with a maximum and minimum of 248.6KJ (in the roof, 27m from the

roadway) and 40.12KJ (in the roof, 3m from the roadway) respectively. In comparison, the elastic strain energy on the roadway roof with a stress release area (Scheme two) is lower, with a maximum of 200.3KJ (in the roof, 27m from the roadway); approximately a 19.4% decrease. The largest decrease of elastic strain energy occurs in the stress release area, at approximately 35.7%.

(3) Variation of plastic zone under impact energy.

The dynamic response of the plastic zone under the action of impact energy is shown in Fig. 9 ~ Fig. 10. The plastic zone of the surrounding rock without a stress release area (Scheme one) is large, the depth of which is at least 9m in both sides and the roof. The plastic zone expands greatly from 0.02 seconds to 0.06 seconds. However, the plastic zone of the surrounding rock with a stress release area (Scheme two) is smaller and expands slowly from the stress release area to both the roadway surface and the deeper rock mass. There is no plastic zone in the surrounding rock 4m~8m from the surface of roadway.

Based on the study of the dynamic responses of vertical stress, elastic strain energy and the plastic zone of the surrounding rock, the dissipation mechanism of impact energy in the structure of a stress release area is revealed. When an impact stress wave S propagates from an impact hypocenter to a stress release area, it will refract and reflect at the surface, producing refracted wave S2 and reflected wave S1. Reflected wave S2 will cause plastic failure to the surrounding rock outside the stress release area, and a portion of the impact energy dissipates in this process. The tensile stress produced by reflected wave S1 and the compressive stress produced by impact stress wave S interact, which results in the reduction of stress outside the stress release area. In the process of refracted wave S2 propagating to the roadway surface through the stress release area , the wave causes dislocation, extrusion and repeated injury of rock blocks and dissipates most of the impact energy since the stress release area is composed of joints and fractures, resulting in great attenuation of the impact stress wave. Therefore, the elastic strain energy on the surrounding rock is reduced, as is the stress in the stress release area.

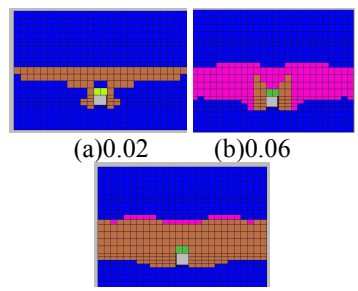

(a)0.02 (b)0.06

(c)0.1s

Fig. 9: Variation of plastic zone in Scheme one.

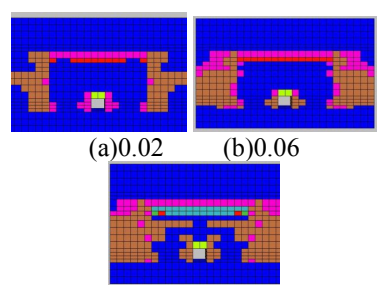

(a)0.02 (b)0.06

(c)0.1s

Fig. 10: Variation of plastic zone in Scheme two.

5. Application Example

5.1 Site conditions and setting of stress releasing area

An intensive impact hypocenter area was monitored in the No. 2304 air return roadway in the Tangkou coal mine by using a microseism monitoring device,

and the intensive area was determined to be in the roof 40m above the roadway. The intensive area is parallel to the floor of the roadway and a little wider, as shown in Fig. 11. The monitoring results show that there is high impact energy in the intensive area and it is impossible to resist the impact of rock-burst with just the initial support and surrounding rock.

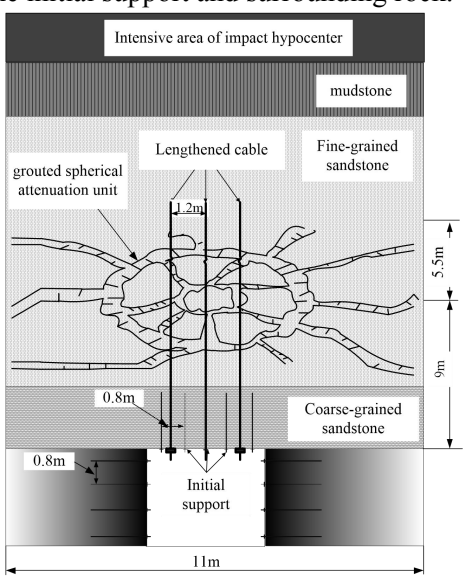

Fig. 11: Structure model of deep roadway rock-burst defense.

To reduce the possibility of rock-burst in the No. 2304 air return roadway, No. 2 rock ammonium nitrate charges were used to conduct coupled blasting. These charges were placed in the roof 9m from the roadway surface every 22m from 138m to 182m along the strike direction of the roadway. The radius was 0.75m, and the structure of the spherical attenuation units after three blasting operations is shown in Fig. 11. Measured by an ultrasonic tester, the widths of the crush zone, rupture zone and fracture zone were 1.2m, 1.9m and 7.9m respectively.

To ensure that these three spherical attenuation units turned into grouted spherical attenuation units, grouting was conducted shortly after blasting. The wave impedance of the grouting material should be $Z_2 = Z_1/2 = 7.1\times10^6 kg\cdot m^{-2}\cdot s^{-1}$ so as to ensure better weakening and strengthening effect. A lengthened cable (16m) was installed shortly after solidification.

The structural model of deep roadway rock-burst defense was formed after drilling blasting, crack grouting and lengthened cable supporting.

5.2 Effect of rock-burst prevention in No. 2304 air return roadway

Due to the stress release area set artificially in the No. 2304 air return roadway, the shock and vibration energy dissipation capability was strengthened and the impact on the supporting system reduced, resulting in a significant improvement in rock-burst prevention capability. There were no rock-burst accidents in the No. 2304 air return roadway from November 2012 to November 2013, and the deformation of the roadway has been very small.

6. Conclusions

(1) There is a crush zone, rupture zone and fracture zone in a stress release area set by artificial blasting, which forms spherical rupture units. The attenuation coefficient of the high energy stress wave that propagates from the intact rock and stress release area to the anchor area was obtained.

(2) The dynamic variation of vertical stress, elastic strain energy and the plastic zone of the surrounding rock under the action of shock and vibration energy were studied using the numerical simulation method, and the dissipation law of shock and vibration energy affected by a stress release area was revealed.

(3) The structural model of deep roadway rock-burst defense was built, and field application shows that setting a stress release area in a deep roadway strengthens the shock and vibration energy dissipation capability and reduces the impact of shock and vibration energy on the supporting system, which significantly improves the capability of rock-burst prevention.

7. Acknowledgments

This research is supported by the National Basic Research Program of China (973 Program, No. 2010CB226805); the Taishan Scholar Construction Project of Shandong Province, China; the National Natural Science Foundation of China (No. 51344009); the Research Award Fund for Outstanding Young Scientists of Shandong Province (No. BS2012NJ007); the Ground Pressure and Strata Control Innovative Team Fund of SDUST (No. 2010KYTD105); and the Shandong Province Natural Science Fund (No. ZR2012EEZ002).

8.References

[1] Hill, R, "A general theory of uniqueness and stability in elastic-plastic solids", Journal of the Mechanics and Physics of Solids, 6(3): 236-249, 1958.

[2] R. G. Morrison, "K. Theory and the practical problem of rock bursts", Engineering and Mining Journal, 149(3): 66-72, 1948.

[3] Huang Gun, Guangzhi Yin, and Xiaoshuang Li, "Effect of Gas Pressure on the Transport Properties of Outburst-Prone Coal", Disaster Advances, 4(3): 20-23, 2011.

[4] Jianguo Ning, Xuesheng Liu, and Yunliang Tan, "Mechanism of Rock-burst Prevention by Synergizing Pressure Relief and Reinforcement of Surrounding Rocks with Zonal Disintegration in Deep Coal Roadway", Disaster Advances, 5(4): 844-850, 2012.

[5] Saharan, Mani Ram, and Hani Mitri, "Destress blasting as a mines safety tool: some fundamental challenges for successful applications", Procedia Engineering, 26: 37-47, 2011.

[6] Baoyao Tang, "Rockburst control using distress blasting", Montreal: McGill University, 2000.

[7] А.Н.Ханукаев, "Physical processes of ore and rock blasting", Beijing: Metallurgical Industry Press, 1980.

[8] Guanshi Wang, Changhong Li, and Shili Hu, "A study of time-and spatial-attenuation of stress wave amplitude in rock mass", Rock and Soil Mechanics, 31(11): 3487-3492, 2010.

[9] Rinehart J S, "Stress transient in solids", Beijing: Coal Industry Press, 1981.

[10] Qi Zhang, "Transfer process of Stress wave at the joints", Journal of Geotechnical Engineering, 8(6): 99-105, 1986.

[11] Xiangfeng Lv, Yishan Pan, and Jupeng Tang, "Similar material simulation test and numerical analysis of impact damage law of roadway under interaction between coal and support", Rock and Soil Mechanics, 33(2): 604-610, 2012.